Nonthermal electron cyclotron emission in marginally stable quiescent runaway electron discharges

Kikyung Park[1], Yeongsun Lee[1], Gunsu Yun[2] and Yong-Su Na[1]*

[1] *Seoul National University, Seoul, Korea,* [2]*POSTECH, Pohang, Korea*

*e-mail: ysna@snu.ac.kr

1. Introduction

Runaway electrons (REs) are a major concern in tokamak disruptions [1]. However, it is difficult to understand the RE physics during the disruption because the rapid evolution of disruption plasmas complicates isolating RE generation, transport and wave-particle interaction from others. Quiescent runaway electron (QRE) discharges provide a more controlled platform, where RE dynamics is relatively stationary and background plasma parameters are better constrained [2].

Despite the opportunity of sufficient acquisition time in QRE plasmas, most diagnostics provide only partial information on the spatial-momentum (6D) space distribution of REs. The reconstruction of the distribution from a finite number of signals is not unique. Among various diagnostics, electron cyclotron emission (ECE) [3, 4] is specialized at probing the perpendicular energy spectrum of suprathermal electrons (roughly with the relativistic factor $\gamma \in (1,2)$) [5]. Nevertheless, quantitative interpretation of ECE alone remains challenging because the signal depends on the unresolved RE distribution through the nonthermal emission and absorption coefficients [5]. Instead of directly inferring the RE distribution from ECE alone, a physics-based RE distribution can be used to calculate the nonthermal emission and absorption coefficients, and the resulting radiative temperature. Indeed, Breizman and Kiramov recently demonstrated that the RE distribution can be characterized when the marginal stability condition is satisfied [6], which might facilitate the model-based measurement.

In this work, we apply a 1D nonthermal synthetic ECE framework to KSTAR QRE discharges in the pre-burst phase. The RE distribution is constructed from the Breizman marginal stability model [6], and the corresponding nonthermal emission and absorption coefficients are implemented in SYNO [7] to calculate the radiative temperature. By comparing the calculated radiative temperature with the measured one in KSTAR, this study evaluates whether the RE distribution constructed from the marginal stability model is consistent with the observed nonthermal ECE behavior.

2. Marginally Stable Runaway Electron Distribution Function

The marginally stable RE distribution adopted in this work follows the Breizman model [6], where the RE distribution is constrained by the balance between kinetic drive and collisional wave damping. This model assumes a continuous whistler wave spectrum, so that the RE distribution is scattered by quasi-linear diffusion over a broad resonance range rather than discrete cavity modes [8]. For anomalous Doppler interaction ($l = -1$), governed by the resonance condition $\omega(k) - k_{\parallel}v_{\parallel} = l|\omega_{ce}|/\gamma$, the marginal condition $\Gamma_b = \Gamma_d$ constrains the parallel momentum dependence of the RE distribution. The balance in the whistler branch yields the perpendicular-momentum-integrated distribution $F(P_{\parallel})$;

$$F(P_{\parallel}) = 2\pi \int_0^{\infty} P_{\perp}\ f(P_{\parallel}, P_{\perp}) dP_{\perp} = \frac{27\nu}{\pi\Omega_{pe}^2}\frac{1}{P_{\parallel}^2} \tag{1}$$

where $P = p/m_e c, \nu = \nu_{ei}/|\omega_{ce}|$ and $\Omega_{pe} = \omega_{pe}/|\omega_{ce}|$. The marginal condition fixes the $P_{\parallel}$ dependence, while the perpendicular dependence is represented by $G(P_{\perp})$ obtained from marginal stability eigenvalue problem. The corresponding two-dimensional distribution is written as

$$f(P_{\parallel}, P_{\perp}) = F(P_{\parallel})\frac{G(P_{\perp})}{2\pi\int_0^{\infty} P_{\perp}\,G(P_{\perp})\,dP_{\perp}} = \frac{27\nu}{\pi\Omega_{pe}^2}\frac{1}{P_{\parallel}^2}\frac{G(P_{\perp})}{2\pi\int_0^{\infty} P_{\perp}\,G(P_{\perp})\,dP_{\perp}}. \tag{2}$$

3. Synthetic ECE Modeling with a Marginally Stable Runaway Electron Distribution

3.1 Phase-space construction of the nonthermal RE distribution

The nonthermal RE distribution is constructed piecewise in $P_{\parallel}$, as illustrated in Figure. 1. The marginal stability solution is applied to the high-P region, where the small angular spread approximation and wave-induced scattering condition are satisfied,

$$P_{min} \equiv \sqrt{\hat{\tau}_{rad}\hat{E}} \ll P_{\parallel} \ll P_{max} \equiv \min\left(\frac{\hat{E}^2\hat{\tau}_{rad}}{Z_{\text{eff}}}, \frac{\sqrt{3M}}{\Omega_{pe}}\right) \tag{3}$$

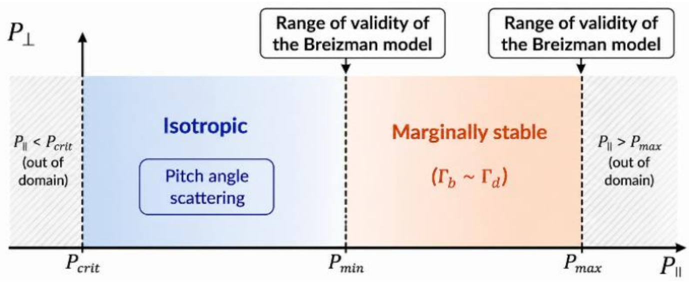

Figure 1. Phase-space model for RE distribution based on marginal stability.

For $P_{\text{crit}} < P_{\parallel} < P_{min}$, where P_{crit} is the critical momentum for runaway acceleration, the marginal stability solution cannot be imposed directly because the small angular spread condition is not satisfied below P_{min}. In this intermediate (suprathermal) region, we infer the particle flux level across P_{min} from the marginally stable region and apply the constant flux from P_{crit} to P_{min} due to the free acceleration feature. The pitch-angle distribution is assumed to be isotropic. This assumption is taken to maximize the nonthermal effect under the given particle flux and determine whether the nonthermal population estimated from the matching is sufficient for accounting for ECE measurements.

3.2 Nonthermal ECE emission and absorption coefficients

The nonthermal ECE calculation follows the effective emission and absorption formulation. For a given electron distribution $f_0(p_{\parallel}, p_{\perp})$, the relevant nonthermal coefficients are

$$j_{\omega} = 2\pi \int dp_{\parallel}\ dp_{\perp}\, p_{\perp}\, \eta_{\omega} f_0(p_{\parallel}, p_{\perp}) \tag{4}$$

$$\alpha_{\omega} = -\frac{8\pi}{3}\frac{c^2}{n_r\omega^2}\frac{\omega}{mc^2}2\pi\int dp_{\parallel}\ dp_{\perp}\,\eta_{\omega}\left[\gamma\omega\frac{\partial f_0}{\partial p_{\perp}} - k_{\parallel}c\left(p_{\parallel}\frac{\partial f_0}{\partial p_{\perp}} - p_{\perp}\frac{\partial f_0}{\partial p_{\parallel}}\right)\right] \tag{5}$$

The single-particle spectral emissivity is

$$\eta_\omega = \frac{\omega\omega_p^2}{p}\frac{1}{8\pi^3 mc^5}\sum_l \frac{E^\dagger \cdot \overleftrightarrow{S_l} \cdot E}{|E_y|^2}\delta(\omega - k_\parallel v_\parallel - l\omega_B) \tag{6}$$

where $\omega_B = \omega_c/\gamma$. These expressions are used as the starting point for calculating the nonthermal contribution from the marginally stable runaway electron distribution.

The nonthermal coefficients are evaluated using the X-mode polarization with $k_\parallel = 0$. The single-particle emission tensor is contracted with the polarization vector, giving

$$\Xi_l \equiv \frac{E^\dagger \cdot S_l \cdot E}{|E_y|^2} = \frac{v_\perp^2}{\tilde{E}_y^2}\left[\frac{l}{\lambda_B}J_l(\lambda_B) - \tilde{E}_y J_l'(\lambda_B)\right]^2 \tag{7}$$

The resonance delta function enforces the cyclotron resonance condition, allowing the $P_\parallel$ integration to be evaluated at the resonant momentum. For $k_\parallel = 0$, this gives

$$\delta\left(\omega_{\mathrm{obs}} - \frac{l\omega_{ce}}{\gamma}\right) = \frac{\gamma_{\mathrm{res}}^2}{\omega_{\mathrm{obs}} P_{\parallel,\mathrm{res}}}\delta(P_\parallel - P_{\parallel,\mathrm{res}}) \equiv J_\delta \delta(P_\parallel - P_{\parallel,\mathrm{res}}). \tag{8}$$

As a result, the original two-dimensional momentum-space integral is reduced to a one-dimensional integral over $P_\perp$. For each harmonic, the nonthermal emissivity and absorption coefficient from the marginally stable runaway electron distribution are written as

$$j_{\mathrm{mRE},l} = C_0 \int_{P_{\perp,min}}^{P_{\perp,max}} dP_\perp \left[P_\perp J_\delta \frac{G(x)}{P_{\parallel,\mathrm{res}}^2}\Xi_l\right] \tag{9}$$

$$\alpha_{\mathrm{mRE},l} = C_\alpha \int_{P_{\perp,min}}^{P_{\perp,max}} dP_\perp \left[P_\perp \gamma_{\mathrm{res}} J_\delta \left(-\frac{2P_\perp}{P_s^2 P_{\parallel,\mathrm{res}}^2}G'(x)\right)\Xi_l\right]. \tag{10}$$

4. Comparison with KSTAR Quiescent Runaway Electron Discharges

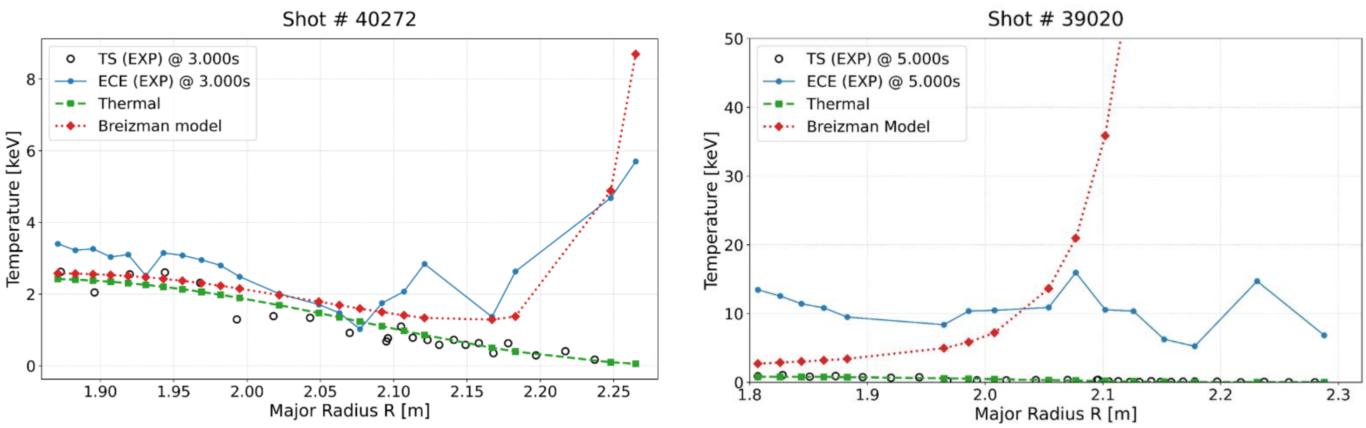

Figure 2. Calculated T_{rad} profiles compared with KSTAR ECE data for #40272 (left) and #39020 (right).

We applied the model to KSTAR and compared the results with the experiment. For shot #40272, the model qualitatively reproduces the nonthermal ECE profile. In the core channels, the reconstructed T_{rad} (red curve) exhibits a finite nonthermal correction on the Maxwellian limit (green curve) although it’s lower than the actual measurements (blue curve). In the edge channels, the model successfully captures the outward increasing trend of the nonthermal ECE response. This indicates that the marginally stable RE distribution can account for the nonthermal ECE response in #40272 within the present modeling assumptions.

The same modeling approach was then applied to another KSTAR QRE discharge, shot #39020, for cross-shot comparison. For shot #39020, the model does not reproduce the radiative temperature profile in the KSTAR ECE data.

The core-edge difference observed in the cross-shot comparison suggests that the model validation is not conclusive yet. One possible explanation is that the model predicts a core RE population that is too small to reproduce the elevated core ECE signal, while the edge contribution may be enhanced through the low-P isotropic region and flux matching. Another plausible mechanism is that the two discharges represent different wave-spectrum regimes. In #40272, the continuous wave spectrum assumption may be supported by a quasi-continuum spectrum potentially seeded by nonlinear parametric decay of slow-X modes [9]. In #39020, a discrete cavity mode might govern the RE dynamics, outside the range of validity of the Breizman model.

5. Conclusion & Discussion

The Breizman marginal stability RE model is applied to KSTAR QRE ECE analysis for the first time. The qualitative agreement in shot #40272 poses the potential that nonthermal synthetic ECE can provide a constraint on the RE distribution in the continuous wave spectrum regime. In contrast, the radial profile of the nonthermal ECE disagrees in #39020, motivating future work to clarify why qualitative agreement is obtained in #40272 but not in #39020. This approach provides a physics-based diagnostic constraint on the RE distribution relevant to wave-particle instability studies. Confirmation of the inferred RE distribution requires additional constraints from complementary diagnostics, such as IR & HXR imaging and wave-spectrum measurements.

Acknowledgement

This research was supported by R&D Program of "Optimal Basic Design of DEMO Fusion Reactor, CN2602-2" through the Korea Institute of Fusion Energy (KFE) funded by the Government funds. This research was supported by the National Research Foundation (NRF) funded by the Korean government (MSIT) (No. RS-2026-25545529). This work was supported by Hyundai Motor Chung Mong-Koo Foundation.

References

[1] B. N. Breizman *et al.*, 2019 *Nucl. Fusion* **59** 083001
[2] C. Paz-Soldan *et al.*, 2014 *Phys. Plasmas* **21** 022514
[3] G. Bekefi 1966. Radiation processes in plasmas. Wiley.
[4] M. Bornatici *et al.*, 1983 *Nucl. Fusion* **23** 1153
[5] C. Liu *et al.*, 2018 *Nucl. Fusion* **58** 096030
[6] B. N. Breizman *et al.*, 2023 *Phys. Plasmas* **30** 022301
[7] Y. Lee *et al.*, 2026 arXiv:2604.26034 (submitted to Phys. Plasmas)
[8] D. A. Spong *et al.*, 2018 *Phys. Rev. Lett.* **120** 155002
[9] Q. Zhang *et al.*, 2026 *Phys. Rev. E* **113** L043203